AIAA 2002-15-2

Preliminary Investigation of Stagnation Point Liquid Injection Influence on Blunt Body Aerodynamics

William C. Woods, Dr. Kenneth M. Jones, and Noah N. Genzel
NASA Langley Research Center
Hampton, VA 23681-2199

AIAA Missile Sciences Conference
5-7 November 2002
Monterey, CA

Preliminary Investigation of Stagnation Point Liquid Injection Influence on Blunt Body Aerodynamics

William C. Woods*, Dr. Kenneth M. Jones†, and Noah N. Genzel‡
Langley Research Center, Hampton, Virginia

Abstract

A preliminary investigation has been performed to determine the influence of stagnation point water injection on the hypersonic aerodynamic forces and moments for two-dimensional blunt bodies. This investigation was performed in the Langley 20-Inch Mach 6 Air Tunnel, and represents the qualitative first phase of a study to examine the potential benefits of water injection to reduce aerodynamic drag and aero-heating. Tests with a 4-inch diameter hemisphere cylinder and a 4-inch diameter cylinder with a span 1.5 times the diameter were performed over a range of free-stream unit Reynolds number from two million to six million per ft and of angle of attack (-5° to 5°) with water and gaseous nitrogen injection at the geometric stagnation point. The momentum flux ratio, that is, the ratio of the momentum flux of the jet to that of the free-stream flow, was varied from the non-blowing value of zero up to 0.00031 by maintaining the jet momentum fixed and varying the free-stream momentum, hence Reynolds number. The effect of water injection on the aerodynamic drag coefficient for the hemisphere cylinder was observed to be negligible as the momentum flux ratio was increased to 0.00017, but decreased significantly as this ratio increased above 0.00017; a nearly 50 percent reduction in drag occurred for a factor of two increase in momentum flux ratio.

Introduction

The effect of mass transfer by blowing or suction on the lifting capability of airfoils (or wings) has been studied for over 50 years. In the late 50's and through the 60's both fluid and gas injection at the stagnation point and around the forward face of entry bodies was experimentally studied for a variety of reasons: radio frequency attenuation, cooling, drag reduction, etc. Mass transfer proved to affect the flow about bodies with resulting changes in pressure distributions, forces, moments, and at supersonic - hypersonic speeds, heating distributions (e. g. references 1 through 6). It may be coincidental, but as ablating heat shields were developed, and adopted, with their natural ability to add mass to the flow field around a blunt body, artificial blowing studies tended to subside except for studies supporting Jovian entry (reference 7 for example) and aerobreaking for orbital plane change (e. g. references 8 through 10).

In the late 70's and early 80's some orbital transfer vehicle designs considered inflatable ballutes for lightweight high drag vehicles. Naturally, aeroheating levels and loads were a major concern. Stagnation point rocket exhaust was considered for both drag modulation and heating reduction. Figure 1, containing figures from references 8 through 10, presents results of stagnation point helium blowing studies performed in the Langley Research Center 22-Inch Mach 20 Helium Tunnel supporting ballute development. Figure 1(a) is a schematic diagram of how the bow shock varies with stagnation point blowing. The solid line shows the bow shock for no blowing. Low blowing produces a fluctuating bulge shown by the large dashed line. Increased blowing produces a large unsteady aerospike that can separate the flow off

* Associate Fellow AIAA, Distinguished Research Associate, Aerothermodynamics Branch
† Senior member, AIAA, Research Engineer, Aerothermodynamics Branch
‡ Student member, AIAA, Cooperative Engineering Student NCSU

the body. Eventually a mass flux balance between the free stream and the jet occurs producing a stable shock structure shown by the small dashed curve. This flow model was observed during the Mach 20 helium tests. Figures 1(b)-(d) summarize the helium results. Drag coefficient, as a function of momentum flux ratio, C_μ, for these flow fields for 90° and 120° included angle bodies and two different expansion ratio nozzles is presented in Fig. 1(b). At $C_\mu \approx 0.01$ drag coefficient is roughly 1/10 the no blowing case ($C_\mu=0$); at $C_\mu \approx 0.03$, C_D was roughly 1/3 to 1/2 the no blowing case depending on the bluntness of the forebody. The focus of these studies at Mach 20 was the hope for high drag, at low fuel consumption, and low heating. At C_μ of 0.03, fuel consumption was excessive. However, additional tests at low blowing conditions indicated reduced pressure in the stagnation region (Fig. 1(c)) and possible surface cooling (Fig. 1(d)). These results indicate the capacity of stagnation point injection to affect drag, pressure, and heating.

In recent years interest has been expressed in atmospheric transit (gun launch) at high initial velocities (30,000 ft/sec at sea level). The severity of this environment (i.e. high heating), and the possibility of deceleration due to high drag losses, has stimulated renewed interest in a basic series of hypersonic experiments to examine the effect of discrete liquid injection at the stagnation point of a blunt body on drag and heating. Due to limited resources, an experimental plan was formulated to provide a qualitative assessment by using simple, easily fabricated bodies and available water pressure to avoid extensive design and fabrication issues associated with complex systems/configurations. (A companion flight experiment was performed in the ballistic range at Eglin Airforce Base).

Nomenclature

α	Angle-of-attack, (degrees)
C_A	Axial force coefficient, (Axial Force/ $q_\infty S_{ref}$)
C_D	Drag coefficient, (Drag/ $q_\infty S_{ref}$)
C_{Do}	Drag coefficient at $\alpha = 0°$
C_N	Normal force coefficient, (Normal force/ $q_\infty S_{ref}$)
C_m	Pitching moment coefficient, (Pitching moment/ $q_\infty S_{ref} l_{ref}$)
C_μ	Momentum flux ratio, ($m_{jet} V_{jet} / \rho_\infty V_\infty^2 S_{ref}$)
l_{ref}	Body diameter (axisymmetric), Body Height (2-D), inches
m	Mass flow, (ρVA), slugs/sec
q_∞	Freestream dynamic pressure ($1/2\, \rho_\infty V_\infty^2$), psi
R	Freestream unit Reynolds Number, ($\rho_\infty V_\infty / \mu_\infty$), 1/ft
S_{ref}	Reference area, base Area, sq. inches
V	Velocity, ft/sec
ρ	Density, slugs/ft^3

Research Apparatus

Models

Desired characteristics for model geometry for the present study include a configuration whose hypersonic flow field and force and moment characteristics are understood; a geometry somewhat inexpensive to machine; and one having a relatively high drag coefficient. Two geometries were selected, a hemisphere cylinder and a quasi two-dimensional cylindrical leading edge slab model with a span 1.5 times the height to achieve near 2-D flow on the centerline. The 2-D cylinder slab model possesses only longitudinal curvature and provides a suitable surface for installing thin film gauges, etched on mylar film, for subsequent heating studies. Both models, fabricated from aluminum, have a 0.020-inch diameter hole drilled at the stagnation point with a 1/8 thick

walled tube bonded to a cavity behind this hole. Flexible tygon tubing was used to provide water at city water pressure (typically 75 psia) to the models. Model size (4-inch diameter) and wind tunnel balance (LaRC WTB HCF-04B) were selected for loads of sufficient magnitude (20 to 80 lbs axial load) to minimize any influence of the water injection system on force measurements (fouling or tare loads). Schematic diagrams of the models (without the water tube) are shown in figure 2. Photographs of the models installed in the test facility are shown in figure 3.

Facility

NASA LARC 20-Inch Mach 6 Tunnel

The NASA Langley 20-Inch Mach 6 Air Tunnel, selected for this investigation, is a blowdown facility with a 20-inch by 20-inch square test section that operates at a fixed Mach number of 6, using dry air as the test medium. Typical test conditions in this facility include nominal freestream unit Reynolds numbers from 0.5 to 9 million/ft. Model angle of attack can be varied in a pitch-pause mode from –5° to 55°, depending upon the length and position of the model in the test section. The design of the injection system permits the pitch-pause sequence at sideslip angles up to 5°. Run times are typically several minutes with a maximum time of approximately 15 minutes. For additional information on this facility see reference 11.

As previously mentioned, to expedite this study, existing city water at constant pressure was utilized (approximately 75 psi). An instant on/off valve, remotely operated from the tunnel control room provided water control and an in line gage measured pressure levels on a run to run and day to day basis to account for variations in city pressure. Accordingly, to vary the momentum flux ratio tunnel test conditions were varied (Reynolds number and free stream momentum) run to run. Table 1 lists test conditions and accompanying momentum flux ratios (C_μ) for both the liquid and gaseous nitrogen spikes produced for each condition.

The test procedure included tare runs with no water injection and tare runs with water injection over the angle-of-attack range. During a tunnel run water was turned on intermittently at each angle to minimize the amount of fluid introduced into the tunnel system. Therefore, at each α, both water off and water on data was obtained. Base pressure was measured and base pressure corrections applied to the axial data.

Discussion of Results

The effect of water injection on the hemi-sphere cylinder flow field is shown in Fig. 4. This is a series of schlieren photographs taken for a range of C_μ from 0 to approximately 0.0003. The initial photograph (Fig. 4(a)) corresponds to no water injection and a unit Reynolds number of 2×10^6/ft, $C_\mu = 0$. Figures 4(b) through 4(e) are schlieren photographs taken at tunnel conditions for Reynolds number of 6×10^6/ft to 2×10^6/ft and water injection pressure of 75 psi resulting in a range of C_μ from approximately .0001 to .0003. Liquid spikes (water spikes as opposed to aerospikes or solid spikes) from 0.16 nose diameter to 1.32 nose diameter in length were produced. In addition, it was observed that the flow field is quite complex and is unsteady. This was not surprising, but since liquid injection tests had not previously been conducted in this tunnel and considering the low pressure environment whether the water would remain liquid or immediately vaporize was unknown. It appears from the schlierens there is a substantial liquid stream and there was no fluid residue in the tunnel after the test.

Figure 5 shows the effect of 5° angle of attack on this complex flow field for R/ft $\approx$ 2×10^6 and $C_\mu \approx 0.0003$. By comparing Figs. 5 and 4(e) ($\alpha = 0°$, $C_\mu \approx 0.0003$) some indication of how angle of attack (i.e., 3 dimensionality) compounds this already complex flow field is gained. Varying the angle of attack from zero significantly reduces the length the water spike is able to extend upstream and the spike takes the form of that observed at zero angle of attack for a lower value of C_μ (compare to Fig. 4(b)).

The effect of water injection on the longitudinal aerodynamic coefficients is shown in Figure 6, where C_A, C_N, and C_m are shown as

functions of angle of attack. As observed in Fig. 6(a) for $C_\mu > 0.0002$ (liquid spikes > 0.3D), a significant reduction in C_A occurs; for example a 45% reduction in C_A occurs at $\alpha = 0°$ as C_μ is increased to 0.00031. Similarly, significant variations occur for both normal and pitching moment as C_μ is increased beyond 0.0002.

The significance of these results is summarized in Fig. 7 where C_{Do} (i.e. C_A at $\alpha = 0°$) is presented as a function of C_μ. For these limited results two distinct linear trends appear. Momentum flux increases from zero (non-blowing) to 0.00016 show little influence on C_{Do}, but a point of departure occurs around $C_\mu \approx$ 0.00016 to 0.00017. For $C_\mu > 0.00016$ a near linear reduction in C_{Do} with C_μ occurs and C_{Do} is reduced to 55% of the no blowing value. The effectiveness of the water spike for drag reduction is clearly indicated.

For comparison purposes limited tests were conducted using dry nitrogen for stagnation point blowing. Figure 8 is a schlieren photograph showing the effect of blowing with nitrogen gas at approximately the same pressure (75 psi) as the water jet and a tunnel free stream unit Reynolds number of 2×10^6/ft. At these conditions the water spike was 1.3 body diameters (Fig. 4(e)). The corresponding nitrogen spike is greatly defuse and only 0.16D in length, even though the momentum flux ratio C_μ is 0.00058; i.e. over approximately 5 times the C_μ value for a comparable water spike (reference Fig. 4(b)). The effect of N_2 blowing on the aerodynamic coefficients (Fig. 9) is about the same as for a water spike of 0.16D corresponding to C_μ=0.00011.

Figure 10 presents schlieren photographs, from the limited tests on the quasi-2D shape showing the effect of water injection on the flow field. The shock stand off distance for the no injection case (Fig. 10(a)) is approximately twice that observed for the hemisphere cylinder (Fig. 4(a)), as expected. These tests were conducted for a tunnel free stream Reynolds number of 2×10^6/ft corresponding to a C_μ = 0.00016. Figure 10(b) shows the effect on the flow field of water injection at a pressure of 75 psia. The water spike length is roughly half the cylinder diameter (0.5D), which is comparable to a water spike for a $C_\mu \approx 0.00016$ to 0.00022 on the axisymmetric (hemisphere cylinder) configuration. For the same Reynolds number and water pressure on the axisymmetric configuration a $C_\mu = 0.00031$ and a water spike of 1.32D occur. The flow appears un-symmetrical; however, the flow is highly unsteady, and this schlieren photograph is at a frozen instant in time. The effect of this flow field on the aerodynamics is shown in Fig. 11. No drag reduction occurs as C_μ is increased from zero to 0.00016, consistent with the axisymmetric results for $C_\mu < 0.0002$. The increase in C_N and C_m is also comparable to the previous results for $C_\mu < 0.0002$.

Future Plans

To provide direct comparison between liquid and solid spikes a series of solid spikes with various fairings at the spike body interface have been fabricated. Testing has been initiated, but results were not available at the time of this publication. Two such configurations are shown in figure 13.

Concluding Remarks

Tests were conducted in the LaRC 20 Inch Mach 6 Air Tunnel using stagnation point water injection for a hemisphere cylinder and quasi 2-D cylindrical leading edge body to examine the effect of geometric stagnation point water injection on the measured aerodynamic coefficients. The influence of water injection on aerodynamic coefficients for the hemisphere cylinder was negligible as the momentum flux ratio was increased to approximately 0.00016 to 0.00017. Aerodynamic drag coefficient decreased significantly as this ratio increased above 0.00017. (A nearly 50 percent reduction in drag occurred for a factor of two increase in momentum flux ratio.) Variation in momentum flux up to 0.00031 produced liquid spikes up to 1.32 times body diameter with drag reduction occurring for liquid spikes greater than 0.3 times body diameter. Limited tests with a quasi 2-D body produced results consistent with those for the hemisphere cylinder. Limited tests with gaseous nitrogen indicated a liquid spike to be

more effective than a gaseous spike, as would be expected.

References

1. Rashis, Bernard: Preliminary Indications of the Cooling Achieved by Ejecting Water Upstream from the Stagnation Point of Hemispherical, 80° Conical, and Flat-Faced Nose Shapes at a Stagnation Temperature of 4,000°F. NACA RM L57103, 1957.

2. Bushnell, Dennis M.; Huffman, Jarret K.: Forward Penetration of Liquid Water and Liquid Nitrogen Injected from an Orifice at the Stagnation Point of a Hemispherically Blunted Body in Hypersonic Flow. NASA TM X-1493.

3. Beckwith, Ivan E.; Bushnell, Dennis M.: Effect of Intermittent Water Injection on Aerodynamic Heating of a Sphere-Cone at Flight Velocities to 18,000 ft per second. NASA TM X-1128, 1965.

4. Beckwith, Ivan E.; Bushnell, Dennis M.; Huffman, Jarret K: Investigation of Water Injection into the Flowfield of the Gemini Vehicle and Predicted Effects on Moments and Communications During Reentry. NASA LWP-84, 1965.

5. Grimaud, John E.; McRee, Leonard: Experimental Data on Stagnation-Point Gas Injection Cooling on a Hemisphere-Cone in a Hypersonic Arc Tunnel. NASA TM X-983, 1964.

6. Charczenko, Nickolai; Hennessey, Katherine W.: Investigation of a Retrorocket Exhausting from the Nose of a Blunt Body into a Supersonic Free Stream. NASA TN D-751, 1961.

7. Holden, Michael S.: An Experimental Study of Massive Blowing from a Nosetip During Jovian Entry. Aerodynamic Research Department , Calspan Corporation Advanced Technology Center, Buffalo, New York. AIAA-81-1070 AIAA 16th Thermophysics Conference, June 23-25, 1981/Palo Alto, California.

8. Grenich, A. F. and Woods, W. C., "Flow Field Investigation of Atmospheric Braking for High Drag Vehicles with Forward Facing Jets in Spacecraft Entry," AIAA Paper 81-0293, AIAA 19th Aerospace Sciences Meeting, St. Louis, MO, January 1981.

9. Andrews, D. G. and Bloetscher, F., "Aerobraked Orbital Transfer Vehicle Definition," AIAA Paper 81-0279, AIAA 19th Aerospace Sciences Meeting, St. Louis, MO, January 1981.

10. Gerald D. Walberg, A Review of Aeroassisted Orbit Transfer (Invited Paper), NASA Langley Research Center, Hampton, VA 23665, Presented at the AIAA 9th Atmospheric Flight Mechanics Conference. AIAA Paper No. 82-1378, San Diego, California, August 9–11, 1982.

11. Miller, C. G., III: Langley Hypersonic Aerodynamic/Aerothermodynamic Testing Capabilities—Present and Future. AIAA CP-90-1376, June 1990.

Table 1

Test Conditions									
P_t, psi	T_t °R	M	R/ft x 10^{-6}	C_μ sphere H_2O	C_μ sphere N_2	C_μ 2-D H_2O	Sphere H_2O spike	Sphere N_2 spike	2-D H_2O spike
125	910	5.97	2	0.00031	0.00058	0.00016	1.320D	0.160D	0.5D
180	910	5.97	3	0.00022			0.720D		
250	910	5.97	4	0.00016			0.340D		
375	935	5.97	6	0.00011			0.160D		

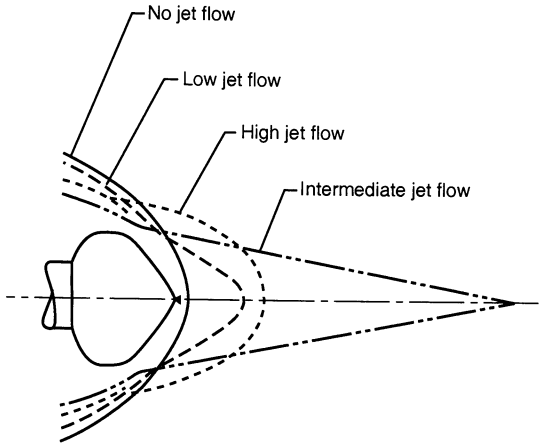

1(a) Changes in bow shock structure due to jet flow.

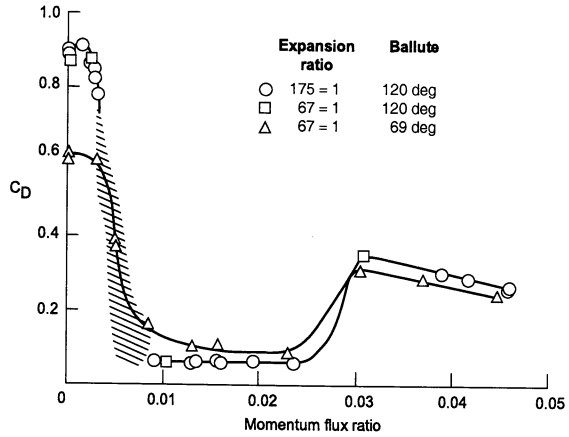

1(b) Variation of drag coefficient with rocket plume momentum flux ballute OTV.

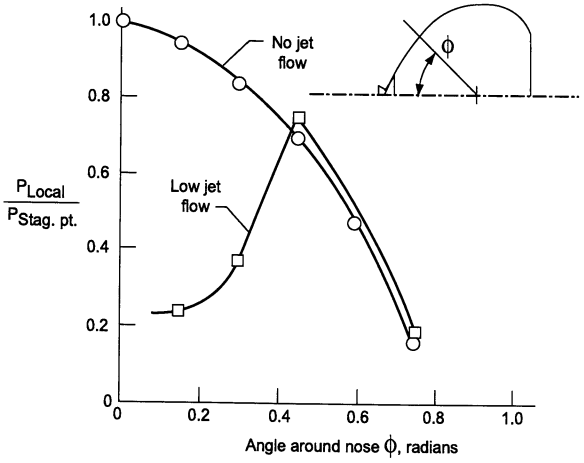

1(c) Effect of jet flow on forebody pressures.

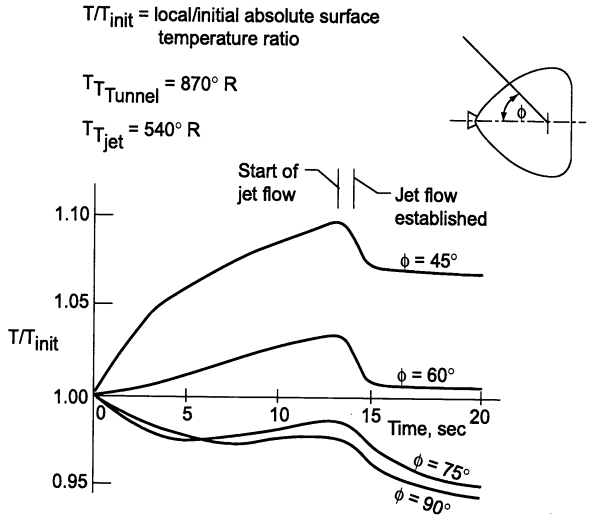

1(d) Effect of jet flow on ballute model surface temperatures.

Figure 1. Effects of stagnation region gas injection for ballute configuration in Mach 20 helium (taken from refs. 8-10).

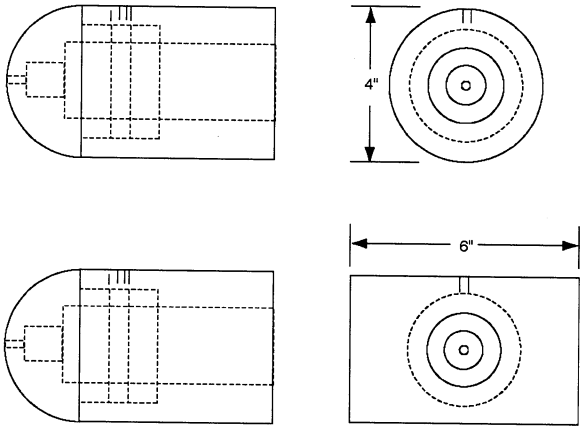

Figure 2. Sketch of the axisymmetric and 2-D models.

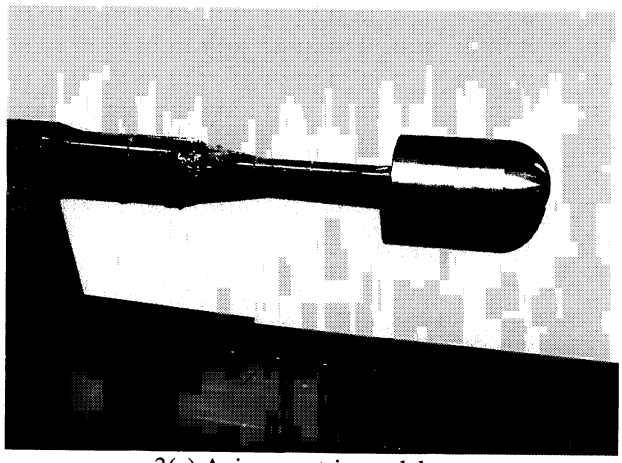

3(a) Axisymmetric model.

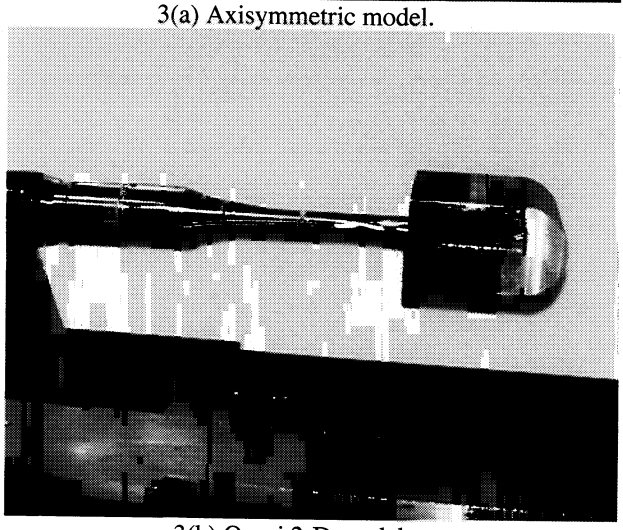

3(b) Quasi 2-D model.

Figure 3. Tunnel installation of models.

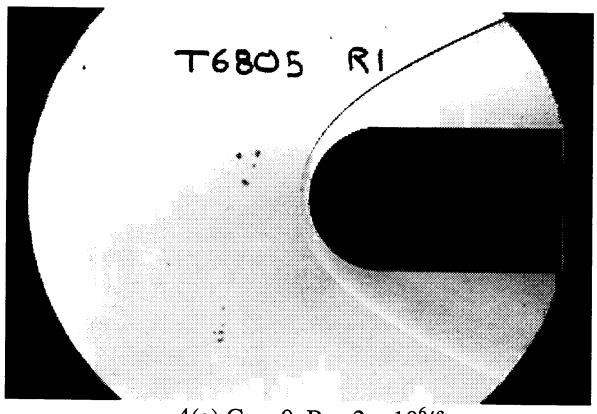

4(a) $C_\mu = 0$, R = 2 x 10^6/ft.

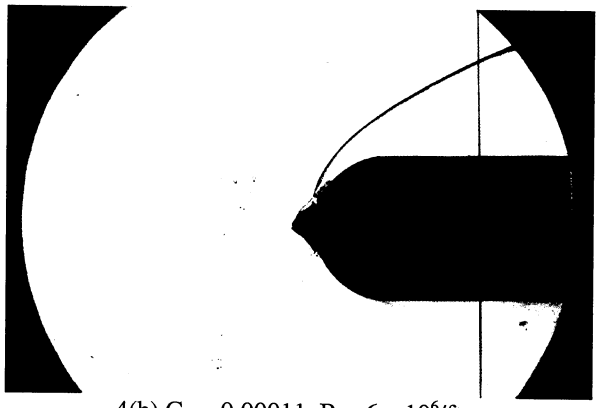

4(b) $C_\mu = 0.00011$, R = 6 x 10^6/ft.

4(c) $C_\mu = 0.00016$, R = 4 x 10^6/ft.

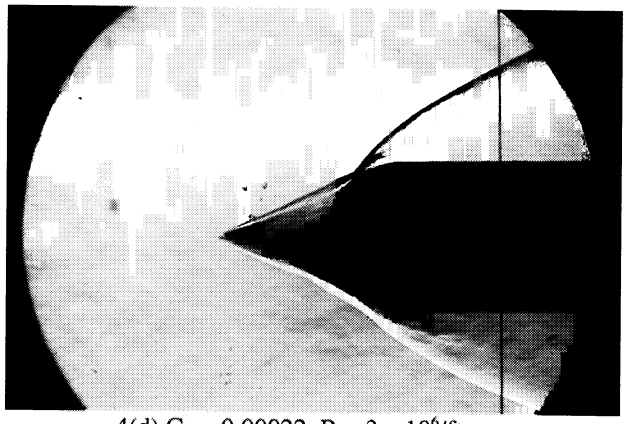

4(d) $C_\mu = 0.00022$, R = 3 x 10^6/ft.

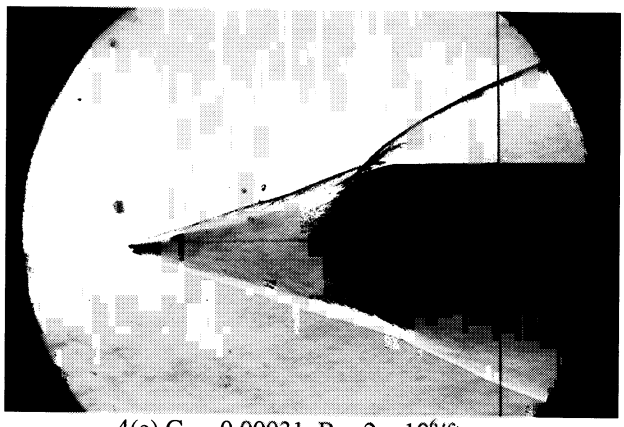

4(e) $C_\mu = 0.00031$, R = 2 x 10^6/ft.

Figure 4. Effect of momentum flux ration for water injection on the axisymmetric model flow field at Mach 6 in air.

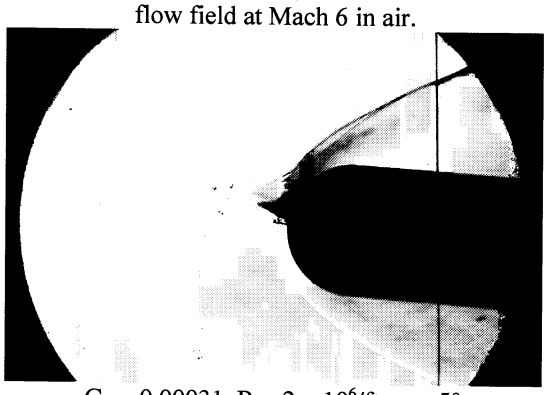

$C_\mu = 0.00031$, R = 2 x 10^6/ft, $\alpha = 5°$

Figure 5. Effect of angle of attack on axisymmetric modelflow field at M = 6 in air with water injection (compare to Fig. 4(e)).

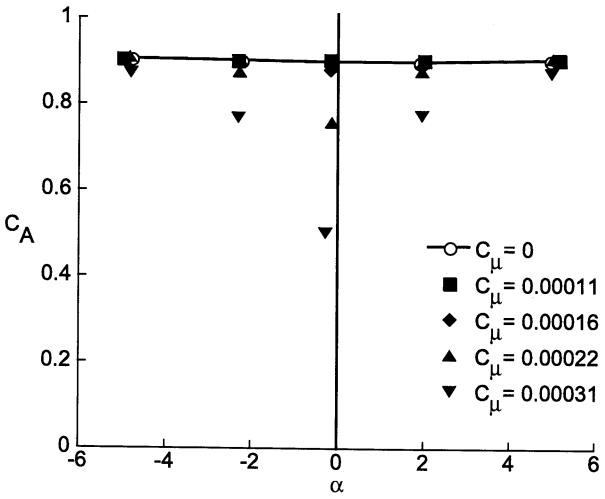

6(a) Effect of C_μ and α on C_A.

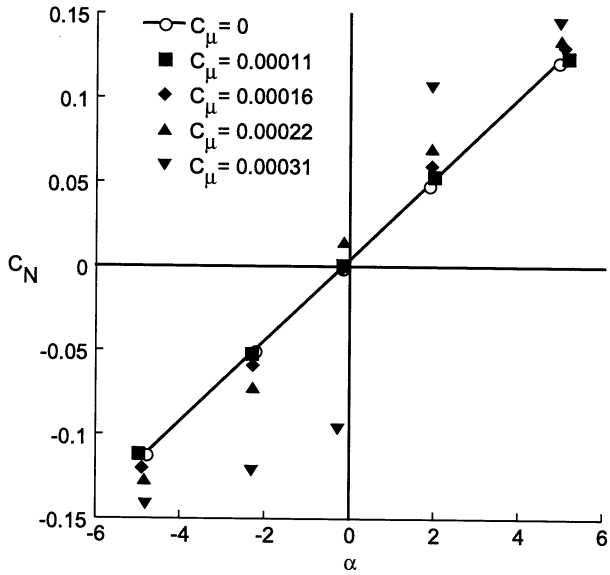

6(b) Effect of C_μ and α on C_N.

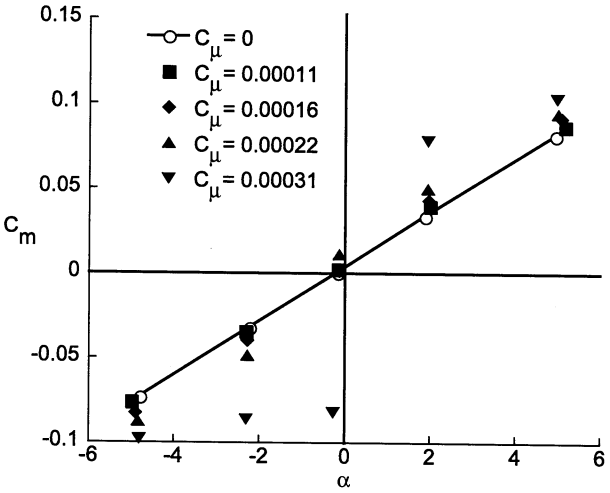

6(c) Effect of C_μ and α on C_m.

Figure 6. Effect of momentum flux ratio and angle of attack on axisymmtric model aerodynamic coefficients at Mach 6.

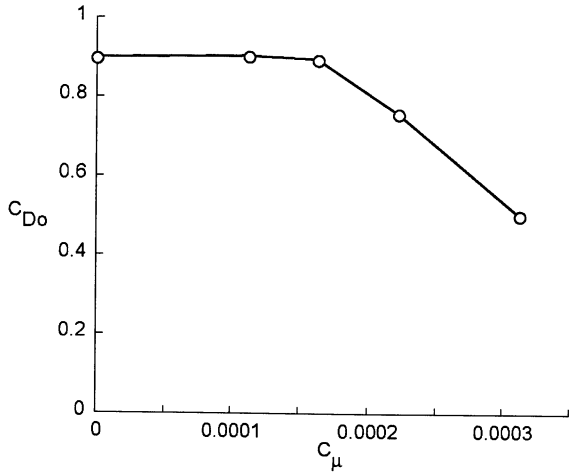

Figure 7. Effect of momentum flux ratio on axisymmetric model $C_{D,0}$ at Mach 6.

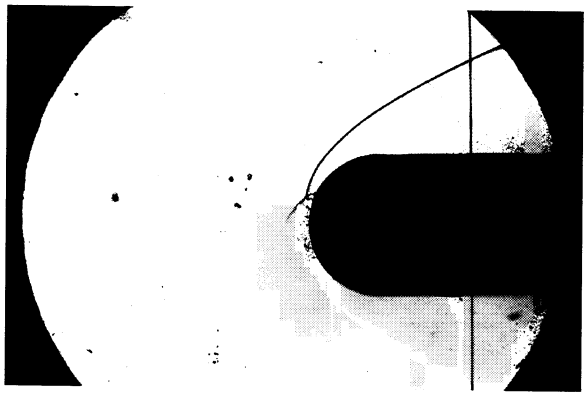

Figure 8. Effect of stagnation point N_2 injection at Mach 6 in air; C_μ = 0.00058, R = 2 x 10^6/ft (compare to Figs. 4 (b), (c)).

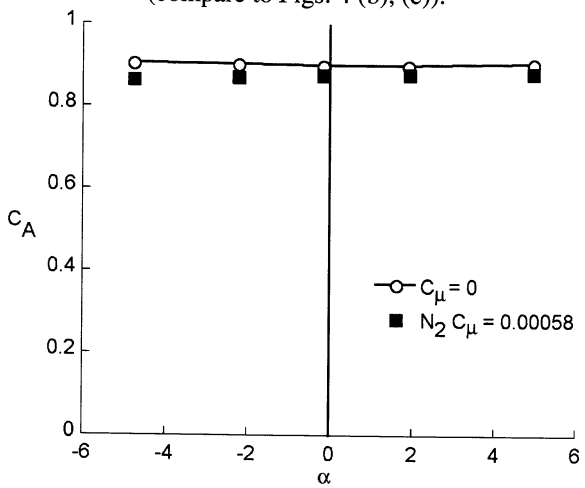

9(a) Effect of C_μ and α on C_A.

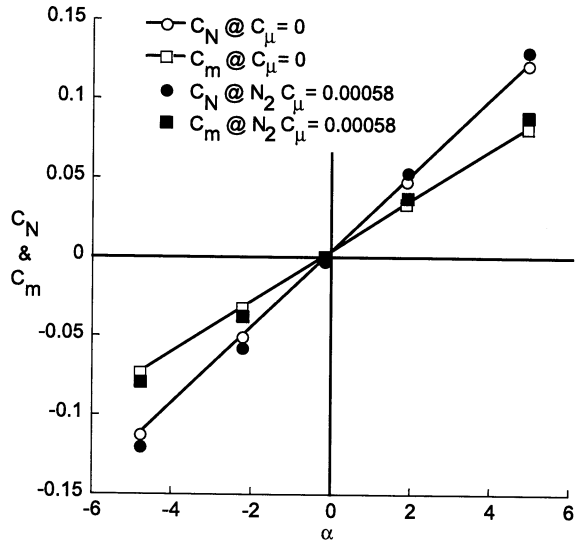

9(b) Effect of C_μ and α on C_N & C_m.

Figure 9. Effect of N2 injection and angle of attack on axisymmetric model aero-coefficients at Mach 6.

10(a) C_μ = 0.

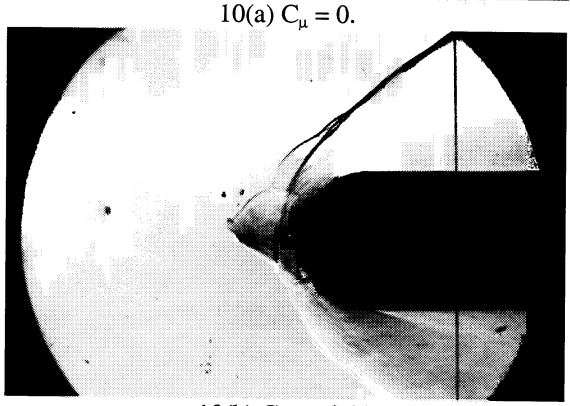

10(b) Cm = 0.00016.

Figure 10. Effect of momentum flux ratio due to water injection on the 2-D model flow at Mach 6, R = 2 x 10^6/ft.

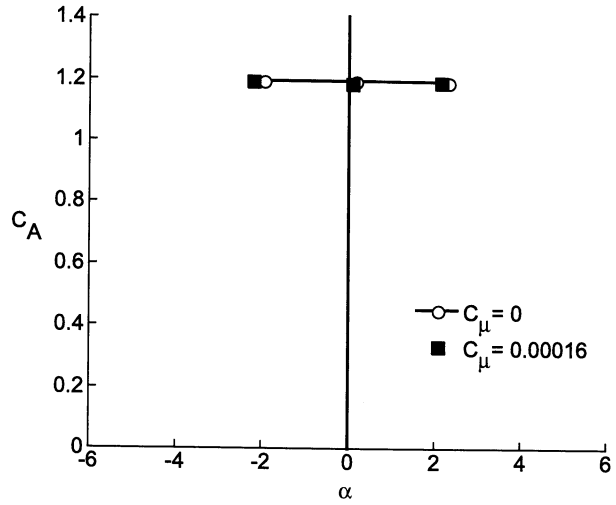

11(a) Effect of C_μ and α on C_A of the 2-D body.

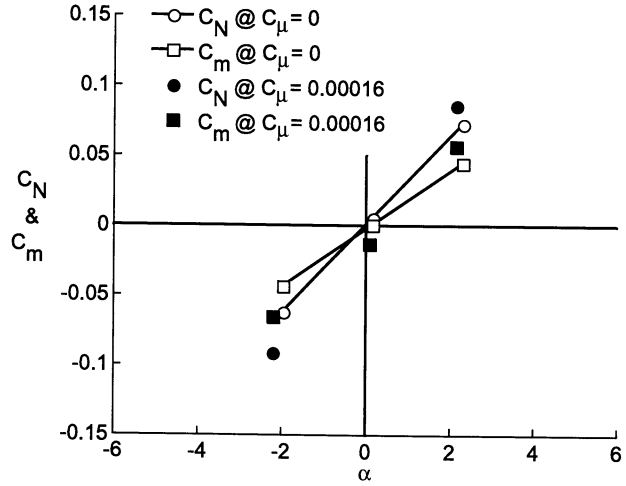

11(b) Effect of C_μ and α on C_N & C_m of the 2-D body.

Figure 11. Effect of water injection and angle of attack on 2-D model aero-coefficients at Mach 6.

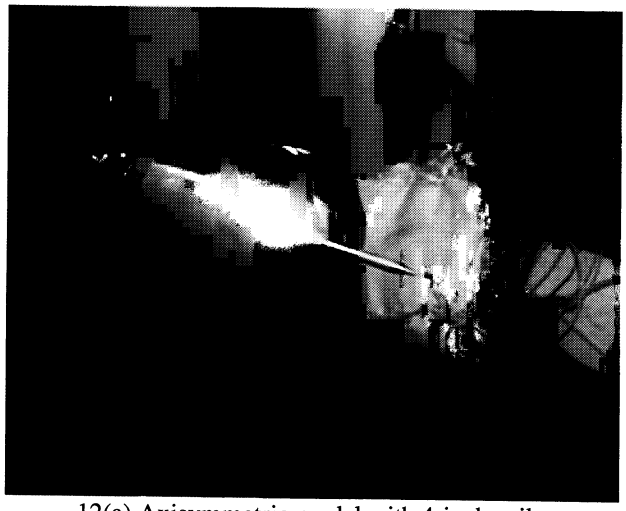

12(a) Axisymmetric model with 4-inch spike.

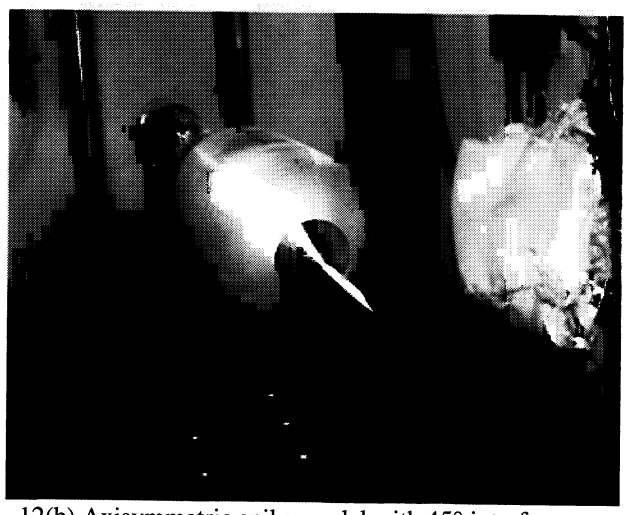

12(b) Axisymmetric spike model with 45° interface.

Figure 12. Tunnel insulation photographs of solid spike models.